Biochemical Pharmacology xxx (2017) xxx–xxx

Contents lists available at ScienceDirect

Biochemical Pharmacology

journal homepage: www.elsevier.com/locate/biochempharm

The pharmacokinetics and metabolism of lumiracoxib in chimeric humanized and murinized FRG mice

A.P. Dickie [a,*], C.E. Wilson [b], K. Schreiter [c], R. Wehr [c], E.M. Wilson [d], J. Bial [d], N. Scheer [e], I.D. Wilson [f], R.J. Riley [a]

[a] Evotec (UK) Ltd, 114 Innovation Drive, Abingdon, Oxfordshire OX14 4RZ, UK
[b] Nestlé Skin Health R&D, Les Templiers, Route des Colles BP 87, F-06902 Sophia-Antipolis, France
[c] Evotec International GmbH, Manfred Eigen Campus, Essener Bogen 7, Hamburg, Germany
[d] Yecuris Corporation, PO Box 4645, Tualatin, OR 97062, USA
[e] CEVEC Pharmaceuticals GmbH, Gottfried-Hagen-Str. 60-62, 51105 Cologne, Germany
[f] Dept. of Surgery and Cancer, Imperial College, London, UK

ARTICLE INFO

Article history:
Received 30 January 2017
Accepted 21 March 2017
Available online xxxx

Keywords:
Reactive intermediates
Taurine conjugation
Glucuronide conjugation

ABSTRACT

The pharmacokinetics and metabolism of lumiracoxib were studied, after administration of single 10 mg/kg oral doses to chimeric liver-humanized and murinized FRG mice. In the chimeric humanized mice, lumiracoxib reached peak observed concentrations in the blood of 1.10 ± 0.08 μg/mL at 0.25–0.5 h post-dose with an AUC_{inf} of 1.74 ± 0.52 μg h/mL and an effective half-life for the drug of 1.42 ± 0.72 h (n = 3). In the case of the murinized animals peak observed concentrations in the blood were determined as 1.15 ± 0.08 μg/mL at 0.25 h post-dose with an AUC_{inf} of 1.94 ± 0.22 μg h/mL and an effective half-life of 1.28 ± 0.02 h (n = 3). Analysis of blood indicated only the presence of unchanged lumiracoxib. Metabolic profiling of urine, bile and faecal extracts revealed a complex pattern of metabolites for both humanized and murinized animals with, in addition to unchanged parent drug, a variety of hydroxylated and conjugated metabolites detected. The profiles obtained in humanized mice were different compared to murinized animals with e.g., a higher proportion of the dose detected in the form of acyl glucuronide metabolites and much reduced amounts of taurine conjugates. Comparison of the metabolic profiles obtained from the present study with previously published data from C57bl/6J mice and humans, revealed a greater though not complete match between chimeric humanized mice and humans, such that the liver-humanized FRG model may represent a useful approach to assessing the biotransformation of such compounds in humans.

1. Introduction

It is widely acknowledged that drug-induced liver injury (DILI) remains a significant cause of attrition in drug discovery [1,2] and a leading cause of acute liver injury in patients that can lead to "Black Box" warnings or drug withdrawals [3–5]. That unexpected failures in the clinic due to DILI still occur despite extensive in vitro and in vivo preclinical safety testing are a potent reminder of the need for better predictive models that translate to humans. A relatively recent example of DILI leading to drug withdrawal is provided by lumiracoxib, [2-(2-chloro-6-fluorophenyl)-amino-5-methylbenzeneacetic acid] (Prexige), developed as a selective COX-2 inhibitor for use in the treatment of osteoarthritis, rheumatoid arthritis and acute pain [6,7]. The drug was removed from the market in most countries after cases of serious liver reactions that included 14 cases of acute liver failure, two deaths, and three liver transplants [8]. Whilst the majority of these only occurred after several months of treatment with lumiracoxib, early presentations were also noted. Many cases involved daily doses exceeding 100 mg, but severe DILI was also reported in those patients who were prescribed 100 mg/day [9,10]. Clues to the cause of this toxicity may have been provided by studies which showed that the drug was bioactivated by peroxidases and human liver microsomes, forming multiple quinone-imine intermediates and glutathione (GSH) adducts indicating the potential for GSH depletion, covalent binding to proteins and oxidative stress etc. [11]. In a recent study in C57bl/6J mice a number of differences between human and murine metabolism of the drug were noted together with some similarities, and there was no evidence of bioactivation.

* Corresponding author.
E-mail address: anthony.dickie@evotec.com (A.P. Dickie).

http://dx.doi.org/10.1016/j.bcp.2017.03.015
0006-2952/

This result suggests that the mouse does not provide an appropriate model for the metabolism and potentially the safety evaluation of lumiracoxib [12]. As a relatively recently developed drug, the withdrawal of lumiracoxib as a result of unexpected DILI, despite having had the benefit of the latest preclinical safety evaluation protocols, provides an eloquent testimony to the need for models (in vitro and in vivo) that translate more accurately to humans. One new model that promises to provide better predictions of human liver-based metabolism (and possible toxicity) is the "chimeric" liver-humanized mouse, where human hepatocytes replace 90 % or more of the murine hepatocytes [13–16]. For example, if the liver toxicity observed in patients was the result of hepatic bioactivation of lumiracoxib, and if chimeric humanized mice accurately reflect metabolism in humans, studies in such mice might have alerted investigators to the potential for hepatotoxicity. Here the pharmacokinetics (PK) and metabolite profile of lumiracoxib in chimeric humanized and murinized FRG mice are described over 24 h following oral administration at 10 mg/kg, and compared to our previous study in normal C57bl/6J mice [12].

2. Materials and methods

2.1. Chemicals

Lumiracoxib was purchased from Selleck Chemicals LLC (supplied by Absource Diagnostics GmbH, Munich, Germany). 2-(2-nitro-4-trifluoro-methylbenzoyl)1,3-cyclohexedione (NTBC) was supplied by Yecuris (Tualatin, OR, USA). Tolbutamide, ammonium acetate and formic acid were purchased from Sigma-Aldrich (Dorset, UK) and leucine enkephalin was supplied by Waters Ltd (Elstree, UK). Analytical grade acetonitrile containing 0.1% formic acid, along with unmodified acetonitrile and methanol, were supplied by Fisher Scientific UK Ltd (Loughborough, UK).

2.2. Animal studies

All animal procedures were performed in accordance with Annex III of the Directive 2010/63/EU applying to national specific regulations such as the German law on animal protection. The PK and the routes, rate of excretion and metabolic fate of lumiracoxib were investigated in 7 male chimeric humanized mice (Hu-FRG™) and 7 male chimeric murinized mice (Mu-FRG™) (30 g), (FRG KO/C57bl/6) (Yecuris (Tualatin, OR, USA)). Following receipt the mice were group housed in cages of up to 3 and maintained under a 12 h light/dark cycle with free access to food and water, and conditions where temperature and humidity were controlled. The animals were initially maintained on 2-(2-nitro-4-trifluoro-methyl benzoyl)-1,3-cyclohexedione (NTBC) for 7 days, then removed from NBTC for 4 weeks prior to the first dose, according to the Yecuris protocol. Before commencing the study a blood sample (25 μL) was taken via the tail vein from each of the humanized mice in order to assess the human albumin concentrations, to ensure that the humanization of the liver was at least ca. 90% according to the Yecuris protocol. Animals were randomized according to body weight and extent of humanization and then allocated to dosing groups. Groups of two Hu-FRG and Mu-FRG mice received dose vehicle (water) whilst each of five Hu-FRG and Mu-FRG was administered lumiracoxib at a nominal dose of 10 mg/kg as a solution in water by oral gavage. Three animals from each group were taken for the determination of the PK of lumiracoxib. Whole blood (20 μL) was collected pre-dose, and 0.25, 0.5, 1, 2, 4, 6, and 8 h post-dose from the tail vein into Minivette POCT K-EDTA coated capillaries and then transferred to 96 well plates, pre-prepared with 20 μL purified water containing 0.2% v/v phosphoric acid, as soon as possible after collection. Gall bladders were taken from this PK group upon sacrifice at 8 h post-dose. The remaining two animals were used to investigate the metabolite profile of lumiracoxib. The animals were placed individually in metabolic cages. Urine and faeces for metabolite profiling from animals dosed with lumiracoxib were collected, over dry ice to ensure sample stability, over 0–8 h and 8–24 h time periods. Urine and faeces from animals dosed with vehicle were collected over dry ice over a 24 h period, and used as controls for metabolite identification. Samples were frozen as soon as possible after collection on dry ice and stored frozen at −80 °C until analysis.

After the final sampling time point (8 h post-dose for the PK group, 24 h post-dose for the metabolite profiling group) the animals were sacrificed by isoflurane inhalation and exsanguination. One aliquot of up to 500 μl of Li-Heparin-plasma was collected (in addition to the microsampling probe). The gall bladder was removed and stored at −80 °C until analysis. In addition, from each animal, small pieces from the left lateral lobe of the liver and a small piece from kidney were weighed and snap frozen at −80 °C into individual Eppendorf tubes as soon as possible after collection.

2.3. Determination of humanization by ELISA

The level of humanization of each mouse was estimated by measuring human albumin in mouse plasma using ELISA (Serum Albumin Human, Abcam # ab179887) according to the manufacturer's protocol. The same assay was performed on terminal plasma samples to assess continuance of liver humanization during the study.

2.4. Quantitative analysis of lumiracoxib in blood

2.4.1. Sample preparation

Aliquots of diluted blood (40 μL) and diluted blood spiked to provide calibration and QC samples were extracted by the addition of 5 volumes (v/v) of cold acidified acetonitrile (ACN) containing 200 nM tolbutamide as an internal analysis standard, mixed vigorously and centrifuged (4566*g*, 20 min) and diluted 1:2 (v/v) with water. A standard curve was prepared at 6 concentrations over the range 30–10,000 ng/mL with QC samples at 3 concentrations over the range 40–4000 ng/mL.

2.4.2. Sample analysis

Analysis of lumiracoxib in blood was performed as described previously (see [12] for details). Briefly, UHPLC-MS/MS using reversed-phase (RP) chromatography with a rapid gradient (1.3 min) was performed on a BEH C18 column (Waters Ltd, Elstree, UK). Mass spectrometric analyses were conducted on an API 6500 triple quadrupole instrument (AB Sciex UK Ltd, Warrington, UK) operating in negative ion electrospray ionisation (ESI) and multiple reaction monitoring modes (MRM) (optimised transition for lumiracoxib was 292 > 248, with declustering potential DP −30 V, entrance potential EP −10 V, collision energy CE −17 V, and collision exit potential CXP −10 V). Non-optimised transitions corresponding to expected metabolites of lumiracoxib were also analysed simultaneously. The instrument was controlled, and data acquired and processed by Analyst™ v.1.6 (AB Sciex UK Ltd, Warrington, UK). Instrument performance (chromatography and response of standards) was assessed before and after sample batch injection to ensure system suitability.

2.4.3. Blood pharmacokinetics

Phoenix WinNonlin 6.4 (Pharsight, Mountain View, CA) was used to generate PK parameter estimates using non-compartmental analysis. Peak (observed) blood concentrations (C_{max}) and AUC_{inf}, as determined by the linear trapezoidal rule

Please cite this article in press as: A.P. Dickie et al., The pharmacokinetics and metabolism of lumiracoxib in chimeric humanized and murinized FRG mice, Biochem. Pharmacol. (2017), http://dx.doi.org/10.1016/j.bcp.2017.03.015

were determined per animal and presented as the mean (n = 2 for humanized mice, n = 3 for murinized mice).

2.5. Metabolite profiling and identification

2.5.1. Sample preparation

In addition to PK analysis, metabolite profiles were determined using aliquots of diluted blood (40 μL) obtained from animals pre-dose and 1, 2 and 4 h post-dose. Samples were extracted by the addition of 4 volumes (v/v) of ACN, vigorous mixing and centrifugation (4566*g*, 20 min) followed by dilution with 1:1 (v/v) with water.

Urine samples obtained for metabolite profiling were pooled by dose group according to weight of urine collected, for each time range (0–8 h and 8–24 h for dosed animals, 0–24 h for vehicle animals). Pooled urine samples were centrifuged (20,800*g*, 5 min) to remove particulates.

Gall bladders removed at 8 h and 24 h from dosed animals were extracted with 8 volumes (w/v) of ACN, mixed vigorously and sonicated for 30 min. The supernatants were pooled by dose group according to weight of gall bladder, centrifuged (20,800*g*, 5 min) to remove particulates and diluted 1:1 (v/v) with water.

Faeces was extracted twice with 3 volumes (w/v) of MeOH:H_2O 1:1 (v/v) and then with 3 volumes (w/v) of MeOH (with centrifugation (4566*g*, 20 min) after each extraction and removal of the supernatant). Aliquots of the combined supernatants from each sample (0–8 h and 8–24 h for dosed animals, 0–24 h for vehicle only mice) were pooled by dose group according to the weight of faeces collected and then evaporated from ca. 1 mL to ca. 200 μL under a stream of dry nitrogen at ambient temperature.

2.5.2. Sample analysis

Metabolite profiles and identities were obtained using a 60 min reversed-phase gradient HPLC-QTOF-MS/MS method that had been developed previously to resolve diclofenac and its murine metabolites [17] and that had recently been applied to lumiracoxib [12] for all of the above sample types. Briefly, 50 μL aliquots of samples were separated on a Hypersil Gold C18 column (Fisher Scientific UK Ltd, Loughborough, UK) with a SecurityGuard C18, 3 μm pre-column filter (Phenomenex Inc., Macclesfield, UK) and eluted over 60 min. The post-column eluent was monitored by both a photodiode array detector (Waters Ltd, Elstree, UK) (monitoring from 210–400 nm at 20 spectra/s) and a Xevo G2 Q-Tof mass spectrometer (Waters Ltd, Wilmslow, UK) operated in positive ion ESI mode. The capillary voltage was set to +500 V, sampling cone to 25 V and extraction cone to 4 V. The source temperature was set to 150 °C, desolvation temperature to 500 °C, the cone gas flow was set to 50 L/h, and the desolvation gas flow to 1000 L/h. Mass spectrometric data were collected in resolution mode, in centroid data format, with a scan time of 1 s and a scan range of 50–1200 Th at a nominal resolution of 30,000. Full scan and product ion mass spectra were acquired simultaneously by HPLC-QTOF-MS^E. Collision energy was applied over a ramp of 20–40 eV for each product ion scan. The instrument was controlled and data acquired by MassLynx™ v.4.1 (Waters Ltd, Wilmslow, UK). Full scan and product ion mass spectra were interrogated by extracting chromatograms of potential metabolites using MassLynx™ v.4.1 from the raw data. Comparison was also made with samples from the appropriate control group (or taken pre-dose) to minimise the potential for false positives from endogenous compounds. The mass spectrometer was calibrated with sodium formate (5 mM) in positive ion mode, and further aligned using an internal lock mass of 2 ng/μL leucine-enkephalin ($[M+H]^+$ 556.2771 Th) infused at 10 μL/min and scanned for 1 s every 57 s. Instrument performance (chromatography, response and mass accuracy of standards) was assessed before and after sample batch injection to ensure data quality. The measured mass accuracy for standards was less than 5 ppm.

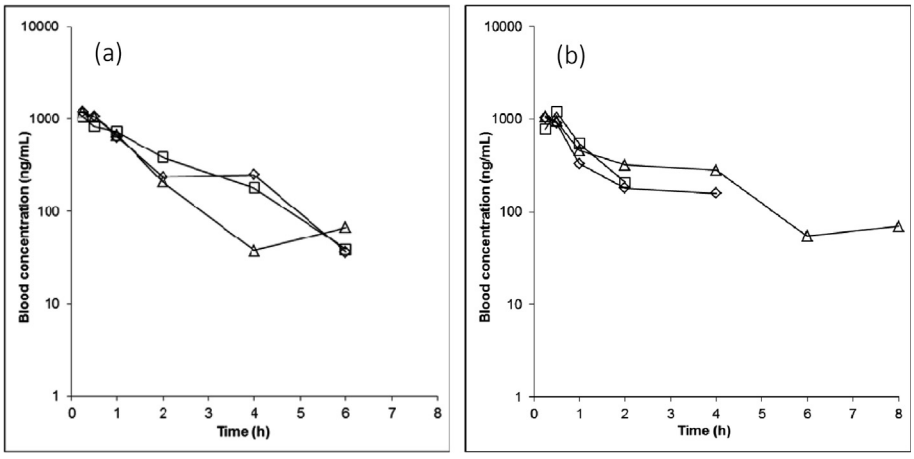

Fig. 1. Blood concentration-time profiles for lumiracoxib following single oral administration at 10 mg/kg to (a) Hu-FRG™ mice (n = 3) and (b) to Mu-FRG™ mice (n = 3). Symbols represent concentration-time profiles from individual animals.

Table 1
Pharmacokinetic parameters for lumiracoxib in C57bl/6, Mu-FRG™ and Hu-FRG™ mice, and [^{14}C]-lumiracoxib in plasma in healthy male subjects.

	Blood C57bl/6 mice*	Blood Mu-FRG™ mice	Blood Hu-FRG™ mice	Plasma healthy male subjects **
Dose (mg/kg)	10	10	10	5.09[a]
C_{max} (μg/ml)	1.26 ± 0.51	1.15 ± 0.08	1.10 ± 0.08	7.28 ± 1.39
t_{max} (h)	0.5 (0.5–1.0)	0.25	0.25 (0.25–0.5)	4.0 (2.5–4.0)
AUC_{inf} (μg.h/mL)	3.48 ± 1.09	1.94 ± 0.22	1.74 ± 0.52	48.4 ± 6.12
$t_{1/2}$ (h)	1.50 ± 0.30	1.28 ± 0.02	1.42 ± 0.72	6.54 ± 1.43

Values are mean ± S.D., except for t_{max} which are median (range).
* Data taken from [12].
** Four subjects received a single 400-mg oral dose of [^{14}C]-lumiracoxib. Using the mean weight of the subjects (78.6 ± 8.8 kg), the dose can be calculated as 5.09 mg/kg [18].

Please cite this article in press as: A.P. Dickie et al., The pharmacokinetics and metabolism of lumiracoxib in chimeric humanized and murinized FRG mice, Biochem. Pharmacol. (2017), http://dx.doi.org/10.1016/j.bcp.2017.03.015

3. Results

3.1. Clinical signs and degree of humanization

There were no clinical observations with all animals behaving normally following oral administration of either vehicle or lumiracoxib at 10 mg/kg. Measurement of human serum albumin (HSA) concentrations in the plasma of the humanized animals indicated that these were >4 mg/mL, consistent with the animals being >90% humanized on days 24 and 29 after removal of NTBC diet.

3.2. Pharmacokinetics of lumiracoxib

The blood concentration versus time profiles for lumiracoxib in the three Hu-FRG™ and three Mu-FRG™ mice are shown in Fig. 1a and b. After administration of the single oral dose (10 mg/kg) of lumiracoxib to Hu-FRG™ mice the drug was rapidly absorbed, with mean peak blood concentrations of 1.10 ± 0.08 μg/mL being reached at approximately 0.25 h (0.25–0.5) post-dose. Good, but variable, exposure was achieved with the mean AUC_{inf} determined as 1.74 ± 0.52 μg h/mL and an apparent mean effective half-life of 1.42 ± 0.72 h (n = 3). Similarly following oral dosing of lumiracoxib (10 mg/kg) to Mu-FRG™ mice rapid absorption was also seen, with mean peak blood concentrations of 1.15 ± 0.08 μg/mL being reached at approximately 0.25 h post-dose. Similar exposure to that seen for the Hu-FRG™ mice was achieved with the mean AUC_{inf} determined as 1.94 ± 0.22 μg h/mL and an apparent mean effective half-life of 1.28 ± 0.02 h (n = 3). In wild type C57bl/6J mice (n = 3) mean peak blood concentrations of ca. 1.3 μg/mL were achieved approximately 0.5 h post-dose (Dickie et al., 2016). In this strain of mouse good, but variable, exposure was achieved with the mean AUC_{inf} determined as ca. 3.5 μg h/mL and an apparent mean plasma terminal half-life of approximately 1.5 h [12]. By way of comparison to healthy human volunteers (n = 4) when lumiracoxib was administered as a single 400 mg dose (ca. 5 mg/kg) peak plasma concentrations were achieved at ca. 4 h post-dose with an apparent mean terminal half-life of ca. 6.5 h [18]. The PK properties of lumiracoxib in wild type C57bl/6J mice [12], Hu-FRG™ and Mu-FRG™ animals and [^{14}C]-lumiracoxib in healthy male subjects [18] are compared to those generated in C57bl/6J mice in the present study in Table 1.

3.3. Lumiracoxib in blood

The only drug-related compound detected in the blood of animals at 24 h post-dose was lumiracoxib itself in trace quantities.

3.4. Lumiracoxib and metabolites in urine

The LC–MS profiles observed for the 0–8 h urine samples from both Hu-FRG™ and Mu-FRG™ mice (Fig. 2a and b) showed the presence of unchanged lumiracoxib but also extensive metabolism to a number of oxidised and conjugated metabolites. In the absence of authentic standards it was not possible to quantify the amounts of each produced, although a qualitative comparison between Hu-FRG™ and Mu-FRG™ mice was possible. The urinary metabolite

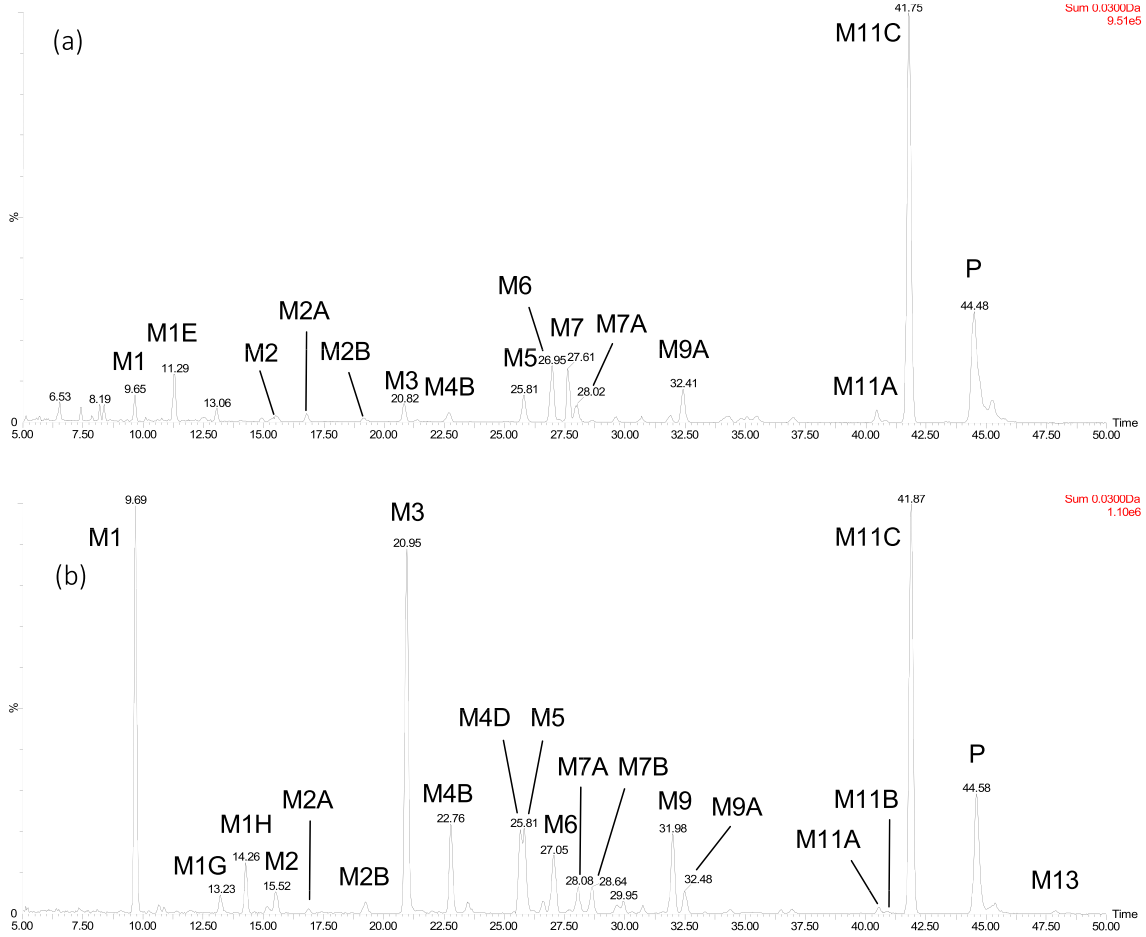

Fig. 2. LC-QTOF-MS profiles of lumiracoxib and its most abundant metabolites in urine 0–8 h following single oral administration of 10 mg/kg lumiracoxib to (a) male Hu-FRG™ mice and (b) male Mu-FRG™ mice.

Please cite this article in press as: A.P. Dickie et al., The pharmacokinetics and metabolism of lumiracoxib in chimeric humanized and murinized FRG mice, Biochem. Pharmacol. (2017), http://dx.doi.org/10.1016/j.bcp.2017.03.015

profiles for both the 8–24 h (data not shown) and 0–8 h collection periods for the Hu-FRG™ mice were similar and dominated by the signal for the acyl glucuronide conjugate **M11C**, (accompanied by smaller amounts of minor transacylated glucuronides such as **M11A/B**). Unchanged lumiracoxib was also detected (possibly in part derived from hydrolysis of the acyl glucuronide) whilst the LC-MS profiles also showed a large number of less intense signals corresponding to a range of hydroxylated, lactamized and

Table 2
Summary of HPLC and mass spectrometric data obtained for lumiracoxib and its metabolites in Hu-FRG™ mouse urine, bile and faeces.

Peak ID	t_R (min)	Assignment	Elemental composition $[M+H]^+$	Theoretical *m/z* /ce:italic> ($^{35}Cl/^{12}C$ isotope $[M+H]^+$)	Observed *m/z* ($^{35}Cl/^{12}C$ isotope $[M+H]^+$)	Δm [observed-theoretical *m/z*] (mDa)
P	44.5	Lumiracoxib	C15H14N1O2Cl1F1	294.0692	294.0699	+0.7
M1	9.7	4′-OH glucuronide	C21H22N1O9Cl1F1	486.0962	486.0964	+0.2
M1A	7.4	4′-OH, 5-COOH	C15H12N1O5Cl1F1	340.0383	340.0391	+0.8
M1B	7.8	4′-OH, 5-COOH indolinone glucuronide	C21H18N1O10Cl1F1	498.0598	498.0606	+0.8
M1C	7.9	OH, 5-COOH	C15H12N1O5Cl1F1	340.0383	340.0392	+0.9
M1D	8.1	OH, 5-COOH indolinone glucuronide	C21H18N1O10Cl1F1	498.0598	498.0599	+0.1
M1E	11.3	5-COOH glucuronide (MNa^+)	C21H19N1O10Cl1F1Na1	522.0573	522.0570	−0.3
M1F	12.5	5-COOH glucuronide (MNa^+)	C21H19N1O10Cl1F1Na1	522.0573	522.0570	−0.3
M2	15.5	4′,5 dihydroxy	C15H14N1O4Cl1F1	326.0590	326.0595	+0.5
M2A	16.8	Unassigned 5-COOH indolinone conjugate	C15H10N1O3Cl1F1	306.0328	306.0343	+1.5
M2B	19.2	5-COOH indolinone glucuronide (MNa^+)	C21H17N1O9Cl1F1Na1	504.0468	504.0459	−1.1
M3	20.8	Unassigned OH indolinone conjugate (MNa^+)	N/A	N/A	477.0659	N/A
M4	21.5	5-COOH	C15H12N1O4Cl1F1	324.0433	324.0446	+1.3
M4A	21.0	OH indolinone	C15H12N1O2Cl1F1	292.0535	292.0524	−1.1
M4B	22.7	OH indolinone	C15H12N1O2Cl1F1	292.0535	292.0542	+0.7
M5	25.8	OH indolinone glucuronide	C21H20N1O8Cl1F1	468.0856	468.0855	−0.1
M6	26.9	5-OH	C15H14N1O3Cl1F1	310.0641	310.0643	+0.2
M6A	27.0	OH indolinone glucuronide (MNa^+)	C21H19N1O8Cl1F1Na1	490.0675	490.0673	−0.2
M7	27.6	5-OH indolinone glucuronide	C21H20N1O8Cl1F1	468.0856	468.0856	0.0
M7A	28.0	OH indolinone glucuronide	C21H20N1O8Cl1F1	468.0856	468.0862	+0.6
M7B	28.6	5-COOH indolinone	C15H10N1O3Cl1F1	306.0328	306.0319	−0.9
M7C	28.6	OH indolinone glucuronide	C21H20N1O8Cl1F1	490.0675	490.0676	+0.1
M8	29.6	4′-OH indolinone glucuronide	C21H20N1O8Cl1F1	468.0856	468.0851	−0.5
M8A	30.6	OH indolinone glucuronide (MNa^+)	C21H19N1O8Cl1F1Na1	490.0675	490.0680	+0.5
M9	31.9	4′-OH	C15H14N1O3Cl1F1	310.0641	310.0643	+0.2
M9A	32.4	OH acyl glucuronide (MNa^+)	C21H21N1O9Cl1F1Na1	508.0781	508.0786	+0.5
M9C	34.3–35.5 (cluster)	OH acyl glucuronide	C21H22N1O9Cl1F1	486.0962	486.0959	−0.3
M10A	36.1	Benzyl, acyl glucuronide (MNa^+)	C20H19N1O8ClF1Na1	478.0675	478.0691	+1.6
M11	37.0	OH indolinone	C15H12N1O2Cl1F1	292.0535	292.0546	+1.1
M11A	40.4	Acyl glucuronide (MNa^+)	C21H20N1O8Cl1F1Na1	492.0832	492.0840	+0.8
M11B	40.8	Acyl glucuronide (MNa^+)	C21H20N1O8Cl1F1Na1	492.0832	492.0824	−0.8
M11C	41.8	1β-O-acyl glucuronide	C21H21N1O8Cl1F1	470.1012	470.1007	−0.5

Please cite this article in press as: A.P. Dickie et al., The pharmacokinetics and metabolism of lumiracoxib in chimeric humanized and murinized FRG mice, Biochem. Pharmacol. (2017), http://dx.doi.org/10.1016/j.bcp.2017.03.015

glucuronidated metabolites. The LC–MS profiles for the 0–8 h urine samples are shown in Fig. 2a. The chromatographic and mass spectrometric properties of these metabolites are provided in Table 2.

In the case of the Mu-FRG™ mice, the most abundant peaks in addition to unchanged parent compound were the 4′-hydroxy ether glucuronide (**M1**) conjugate, an unassigned hydroxy-indolinone metabolite (**M3**) and the acyl glucuronide **M11C** (and its transacylation products (**M11A/B**) (see Fig. 2b). A large number of oxidised metabolites were also present, including the ring oxidised 4′-hydroxy metabolite **M9** (and its ether glucuronide conjugate **M1**), hydroxylation of the 5-methyl group (**M6**), and a 4′, 5-dihydroxylated metabolite (**M2**). As well as the 4′-hydroxy-glucuronide, hydroxy-glucuronides of the indolinone were also seen (**M4C**, **M5/5A**, **M6A**, **M7/7A/7C**, **M8/8A**). These are assumed to be derived from 4′- and 5-hydroxy metabolites due to the prevalence of hydroxylation at these positions. However, for the hydroxy-indolinone metabolites these assignments, based on limited fragmentation data, were not conclusive. In contrast to Hu-FRG™ mice several taurine conjugates were also detected in the urine of Mu-FRG™, including that of the 4′- or 5-hydroxylated metabolite (**M10**), a side-chain shortened benzyl metabolite (**M12**) and the taurine conjugate of lumiracoxib itself (**M13**). The 8–24 h urine also contained a similar range and abundance of metabolites based on signal response (data not shown).

From these results it would appear that the humanized mouse produced a number of metabolites not seen in wild type mouse, notably the acyl glucuronide conjugate (**M11C**), and with some similarities to the profile seen in humans [18]. Interestingly, murinized mice shared similarities with both wild type and humanized mice, exhibiting 4′-hydroxy-ether glucuronide (**M1**) and acyl glucuronide (**M11C**) conjugates as principal urinary metabolites.

For comparison, the major metabolites detected in the urine of C57bl/6J mice (based on signal intensity) after dosing with lumiracoxib were the 4′-hydroxy ether glucuronide conjugate (**M1**), 4′,5-dihydroxylated lumiracoxib (**M2**), an unassigned hydroxy-indolinone (previously thought to be a taurine conjugate) metabolite (**M3**) and 5-hydroxylumiracoxib (via oxidative metabolism of the methyl group) (**M6**) [12]. The metabolite information is provided in Table 3, including a comparison with the wild-type mouse study [12] and the human volunteer study [18].

Table 3
Summary of HPLC and mass spectrometric data obtained for lumiracoxib and its metabolites in Mu-FRG™ mouse urine, bile and faeces.

Peak ID	t_R (min)	Assignment	Elemental composition $[M+H]^+$	Theoretical m/z ($^{35}Cl/^{12}C$ isotope $[M+H]^+$)	Observed m/z ($^{35}Cl/^{12}C$ isotope $[M+H]^+$)	Δm [observed-theoretical m/z] (mDa)
P	44.6	Lumiracoxib	C15H14N1O2Cl1F1	294.0692	294.0694	+0.2
M1	9.7	4′-OH glucuronide	C21H22N1O9Cl1F1	486.0962	486.0965	+0.3
M1C	8.0	OH, 5-COOH	C15H12N1O5Cl1F1	340.0383	340.0397	+1.4
M1G	13.2	Unassigned 5-COOH conjugate	C15H12N1O4Cl1F1	324.0433	324.0438	+0.5
M1H	14.3	Unassigned OH conjugate (MNa^+)	N/A	N/A	493.0616	N/A
M2	15.6	4′,5 dihydroxy-	C15H14N1O4Cl1F1	326.0590	326.0602	+0.7
M2A	16.9	Unassigned 5-COOH indolinone conjugate	C15H10N1O3Cl1F1	306.0328	306.0334	+0.6
M2B	19.2	5-COOH indolinone glucuronide (MNa^+)	C21H17N1O9Cl1F1Na1	504.0468	504.0462	−0.6
M3	21.0	Unassigned OH indolinone conjugate (MNa^+)	N/A	N/A	477.0658	N/A
M4A	20.4	OH indolinone	C15H12N1O2Cl1F1	292.0535	292.0530	−0.5
M4B	22.8	OH indolinone	C15H12N1O2Cl1F1	292.0535	292.0535	0.0
M4C	23.5	OH indolinone glucuronide	C21H20N1O8Cl1F1	468.0856	468.0855	−0.1
M4D	25.7	Unassigned OH indolinone conjugate	N/A	N/A	414.1046	N/A
M5	25.9	OH indolinone glucuronide	C21H20N1O8Cl1F1	468.0856	468.0864	+0.8
M5A	26.6	OH indolinone glucuronide	C21H20N1O8Cl1F1	468.0856	468.0854	−0.2
M6A	27.0	OH indolinone glucuronide (MNa^+)	C21H19N1O8Cl1F1Na1	490.0675	490.0686	+1.1
M6	27.2	5-OH	C15H14N1O3Cl1F1	310.0641	310.0653	+1.2
M7	27.7	5-OH indolinone glucuronide	C21H20N1O8Cl1F1	468.0856	468.0854	−0.2
M7A	28.1	OH indolinone glucuronide	C21H20N1O8Cl1F1	468.0856	468.0855	−0.1
M7B	28.6	5-COOH indolinone	C15H10N1O3Cl1F1	306.0328	306.0338	+1.0
M8	29.7	4′-OH indolinone glucuronide	C21H20N1O8Cl1F1	468.0856	468.0853	−0.3
M8A	30.8	OH indolinone glucuronide (MNa^+)	C21H19N1O8Cl1F1Na1	490.0675	490.0674	−0.1
M9	32.0	4′-OH	C15H14N1O3Cl1F1	310.0641	310.0645	+0.4
M9A	32.5	OH acyl glucuronide (MNa^+)	C21H21N1O9Cl1F1Na1	508.0781	508.0786	+0.5
M9B	34.4	Unassigned OH indolinone conjugate (MNa^+)	N/A	N/A	494.0992	N/A
M9C	34.4–35.4 (cluster)	OH acyl glucuronide	C21H22N1O9Cl1F1	486.0962	486.0981	+2.9
M10	35.9	OH taurine	C17H19N2O5Cl1F1S1	417.0682	417.0662	−2.0
M10A	36.2	Benzyl, acyl glucuronide (MNa^+)	C20H19N1O8ClF1Na1	478.0675	478.0699	+2.4
M11	37.0	OH indolinone	C15H12N1O2Cl1F1	292.0535	292.0538	+0.3
M11A	40.6	Acyl glucuronide (MNa^+)	C21H20N1O8Cl1F1Na1	492.0832	492.0844	+1.2
M11B	40.9	Acyl glucuronide (MNa^+)	C21H20N1O8Cl1F1Na1	492.0832	492.0835	+0.3
M11C	41.9	1β-O-acyl glucuronide	C21H21N1O8Cl1F1	470.1012	470.1020	+0.8
M12	42.1	Benzyl, taurine	C16H17N2O4Cl1F1S1	387.0576	387.0577	+0.1
M13	47.9	Taurine	C17H19N2O4Cl1F1S1	401.0733	401.0732	−0.1
M13A	49.5	Unassigned conjugate	N/A	N/A	470.0708	N/A

Please cite this article in press as: A.P. Dickie et al., The pharmacokinetics and metabolism of lumiracoxib in chimeric humanized and murinized FRG mice, Biochem. Pharmacol. (2017), http://dx.doi.org/10.1016/j.bcp.2017.03.015

3.5. Metabolite profiles of lumiracoxib in bile

The LC–MS profiles observed for the 8 h bile samples from both male Hu-FRG™ and Mu-FRG™ mice (Fig. 3) showed the presence of a number of oxidised and conjugated metabolites. The biliary metabolite profile for the Hu-FRG™ mice was dominated by the 4′-hydroxy ether glucuronide conjugate (**M1**), whereas the Mu-FRG™ mice contained hydroxyl-lactam metabolites (**M3**, **M4A/B**) in addition to the 4′-hydroxy ether glucuronide conjugate (**M1**). The metabolite information is provided in Tables 2 and 3. Metabolite profiles (not shown) for the bile samples obtained at 24 h post-dose from the humanized mice contained only traces of 4′-hydroxy ether glucuronide conjugate, whereas those for the murinized mice also contained traces of the hydroxy lactam metabolites in addition to the 4′-hydroxy ether glucuronide conjugate.

3.6. Metabolite profiles of lumiracoxib in faecal extracts

Faecal extracts produced a less rich metabolic profile for lumiracoxib than either urine or bile. The profiles from both Hu-FRG™ and Mu-FRG™ mice for 0–8 h contained only the presence of low concentrations of unchanged parent and are therefore not presented. The 8–24 h faecal metabolite profile from Mu-FRG™ mice (Fig. 4b) contained the 4′,5-dihydroxy and 5-carboxy-metabolites (**M2** and **M4** respectively), together with lumiracoxib itself. The metabolites contained in the profile obtained from the 8–24 h faecal extract for the Hu-FRG™ mice (Fig. 4a) contained a relatively strong signal for unchanged lumiracoxib peak, the further oxidised 4′-hydroxy, 5-carboxy metabolite (**M1A**), and 5-carboxy lactam (**M1F**) plus the two metabolites (**M2, M4**) seen in murinized faeces. These results are summarized in Tables 2 and 3 and illustrated in Fig. 4.

4. Discussion

The present studies reveal the complexity of the metabolic fate of lumiracoxib in both humanized Hu-FRG™ and Mu-FRG™ mice, involving a broad range of oxidative functionalization reactions, lactamizations and conjugations as summarized in Tables 2 and 3 and depicted in Figs. 5 and 6. Some of these metabolites were already reported as common to both humans and C57bl/6J mice [18,12] and, as expected, the excreta of both the chimeric Hu-FRG™ and Mu-FRG™ mice shared a number of metabolites (to facilitate comparison these metabolite profiles are summarized in a heat map, or "Metmap" in Table 4). Indeed, in all three types of mouse models and humans, in addition to lumiracoxib, the "universally" detected metabolites included the 4′-, 5- mono- (**M9**, **M6**) and 4′,5-di- (**M2**)-hydroxylated metabolites, the product of the subsequent oxidation of the 5′-hydroxy metabolite to the carboxylic acid (**M4**), a lactamized hydroxy-indolinone (**M11**) and the 4′-hydroxy indolinone glucuronide (**M8**).

In general, the metabolites detected in the chimeric Hu-FRG™ animals showed a good correspondence with all of the major metabolites previously found in humans, with the exception of the sulfate conjugates of a hydroxylated carboxylic acid (**H2**) and its lactam (**H4**/**H6**), and a number of 4-OH, 5-COOH indolinone-

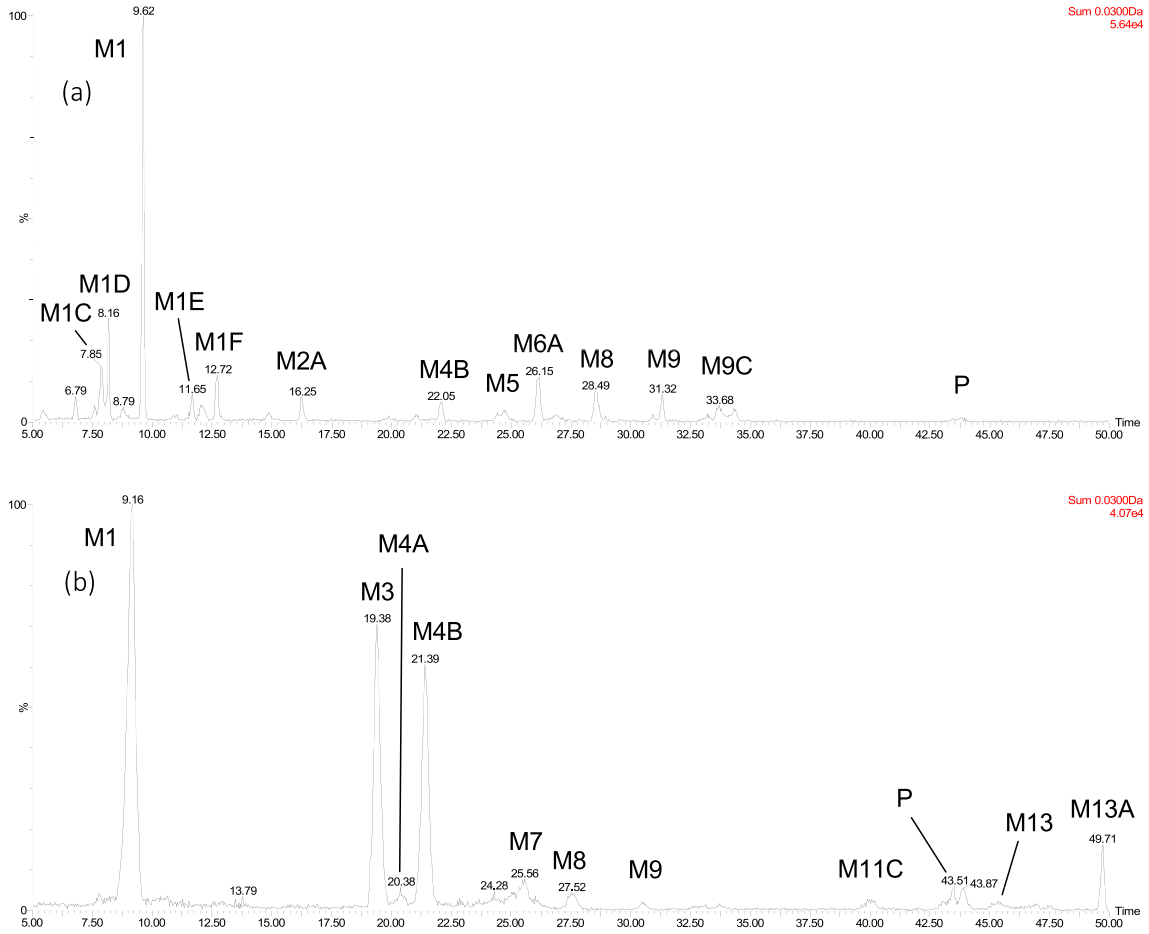

Fig. 3. LC-QTOF-MS profiles of lumiracoxib and its most abundant metabolites in bile 8 h following single oral administration of 10 mg/kg lumiracoxib to a) Hu-FRG™ or b) Mu-FRG™ male mice.

Please cite this article in press as: A.P. Dickie et al., The pharmacokinetics and metabolism of lumiracoxib in chimeric humanized and murinized FRG mice, Biochem. Pharmacol. (2017), http://dx.doi.org/10.1016/j.bcp.2017.03.015

related metabolites (**H8**, **H12**, **H13**), which were not detected in any of the mouse samples examined. Some of the observed differences between humans and Mu-FRG™ mice would seem to reflect a greater degree of conjugation by the Hu-FRG™ animals removing metabolites, e.g., the 4′-OH, 5-COOH lactam (**H8**), by glucuronidation (**M1B**). The reason for the absence of sulfate metabolites in samples derived from the humanized mice Hu-FRG™ mice is not clear. However, it is quite possible that the origin of the sulfate conjugates in humans was both species-specific and extrahepatic and, as only the liver of the Hu-FRG™ was humanized such a metabolite would not readily be formed. Interestingly, from the point of view of extrahepatic metabolism, when the AUC for lumiracoxib in the C57bl/6J wild type animals is compared to that of the FRG™ mice it is seen to be ca. 2-fold higher than that of either strain of chimeric mice whereas the terminal half- life of the drug was similar for all strains (see Table 1). If the assumption is made that the fraction of the dose absorbed was the same for both C57bl/6J and FRG™ mice, the lower exposure of the latter to lumiracoxib is more likely to be due to higher clearance through first pass metabolism during absorption through the gut wall, perhaps as a result of enzyme induction but, as this was not measured, this is clearly speculative. In terms of unique mouse metabolites it is perhaps noteworthy that both Mu-FRG™ and C57bl/6J mice produced a range of taurine conjugates (**M10**, **M12**, **M13**), none of which were seen in either the human radiolabelled study or Hu-FRG™ mice.

The intramolecular cyclisation of lumiracoxib metabolites, with concurrent lactam formation to give a range of indolinones, resulted in the production of a large number of structures, many of which went on to be further transformed by conjugation to e.g., glucuronides (or sulfates in man). It has been suggested that this type of metabolic reaction, which has also been noted for the structurally-related NSAID diclofenac, occurs via the dehydration of the carboxylic acid and intramolecular lactam formation [19,20]. The involvement of S-acyl-CoA-thioester (also required for amino acid conjugations such as those with e.g., taurine as seen here) in indolinone formation has also been suggested [21]. In the case of diclofenac, indolinone formation has also been shown to occur in aqueous solution under appropriate conditions [19] as well in biological fluids (e.g., rat urine [22] and bile [21]).

Conversion of lumiracoxib to indolinones has been described also in in vitro incubations with human liver microsomes [11]. The Mu-FRG™ mice produced the most prolific range of metabolites, including some unique conjugates (e.g., **M1G**, **M1H**, **M5A**, **M9B** and **M13A**) whilst others were shared with both Hu-FRG™ and C57bl/6J mice, such as the side chain shortened benzyl metabolite as either taurine (C57bl/6J mice) or glucuronide (Hu-FRG™ animals) conjugates. This decarboxylation reaction, which has been suggested as a potential means of forming reactive metabolites, has also been observed for diclofenac [23]. Interestingly, in the same way that we have suggested above that taurine conjugation may represent a mouse liver-specific biotransformation, the small amount of the side-chain shortened benzyl-metabolite, detected here as the glucuronide, in the Hu-FRG™ mice, but not (to date) in humans, may well provide complementary information on aspects of residual mouse-specific oxidative metabolism.

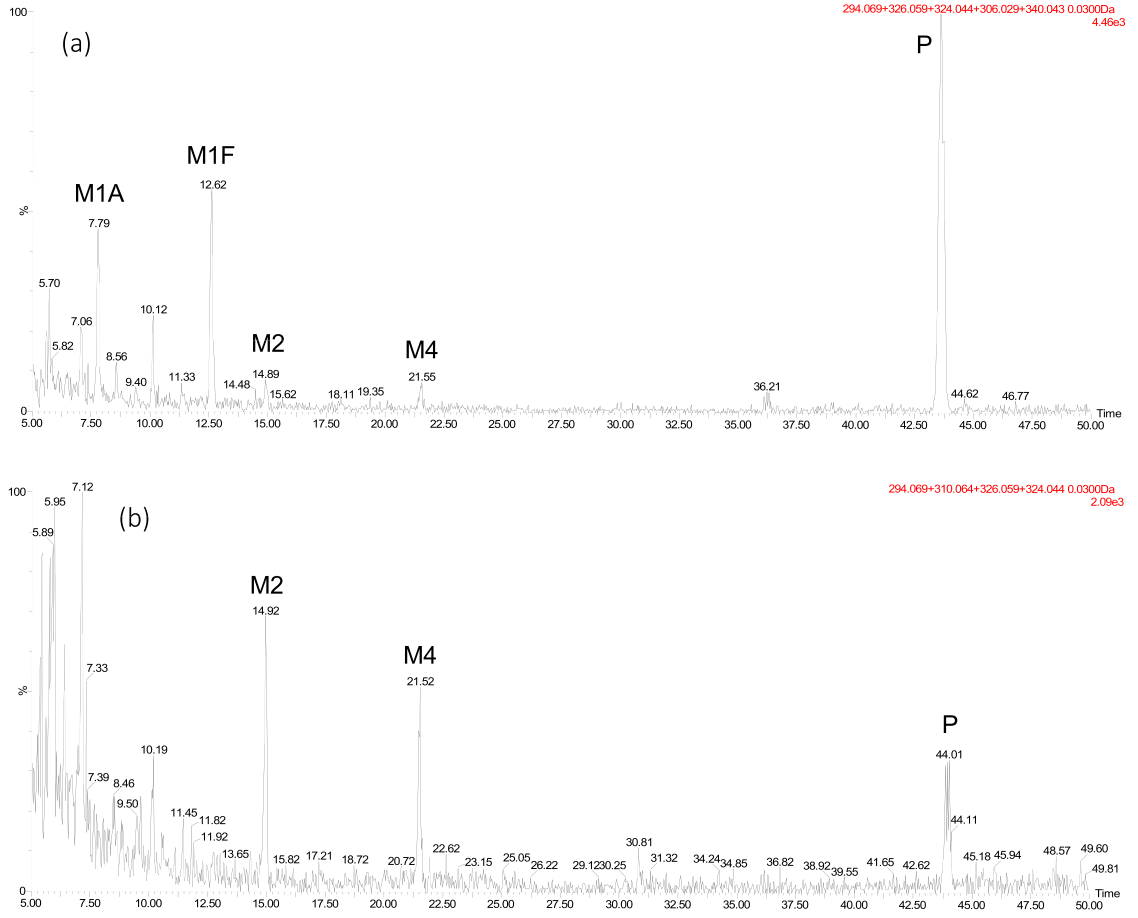

Fig. 4. LC-QTOF-MS profiles of lumiracoxib and its most abundant metabolites in faeces 8 24 h following single oral administration of 10 mg/kg lumiracoxib to a) Hu-FRG™ or b) Mu-FRG™ male mice.

Please cite this article in press as: A.P. Dickie et al., The pharmacokinetics and metabolism of lumiracoxib in chimeric humanized and murinized FRG mice, Biochem. Pharmacol. (2017), http://dx.doi.org/10.1016/j.bcp.2017.03.015

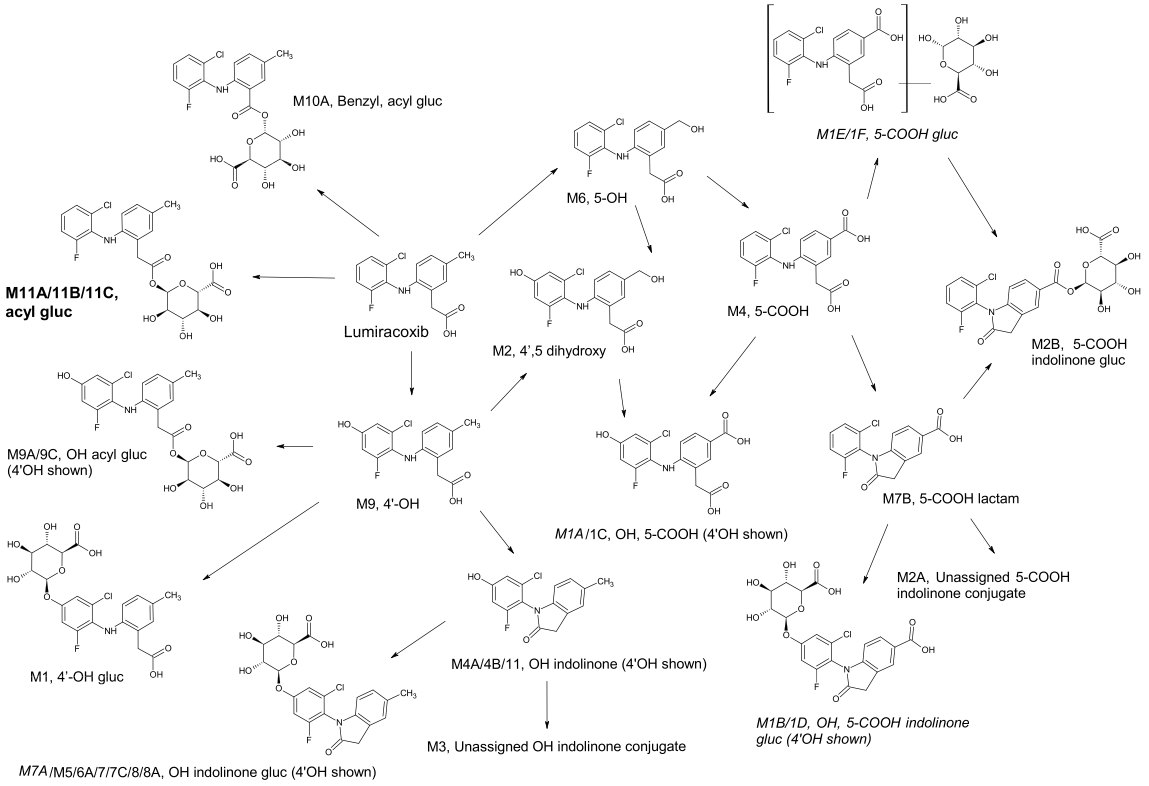

Fig. 5. Proposed metabolic pathway of lumiracoxib in Hu-FRG™ mice. Principal metabolites are designated with large bold font. Metabolites found in Hu-FRG™ mice but not in Mu-FRG™ mice are designated with italic font.

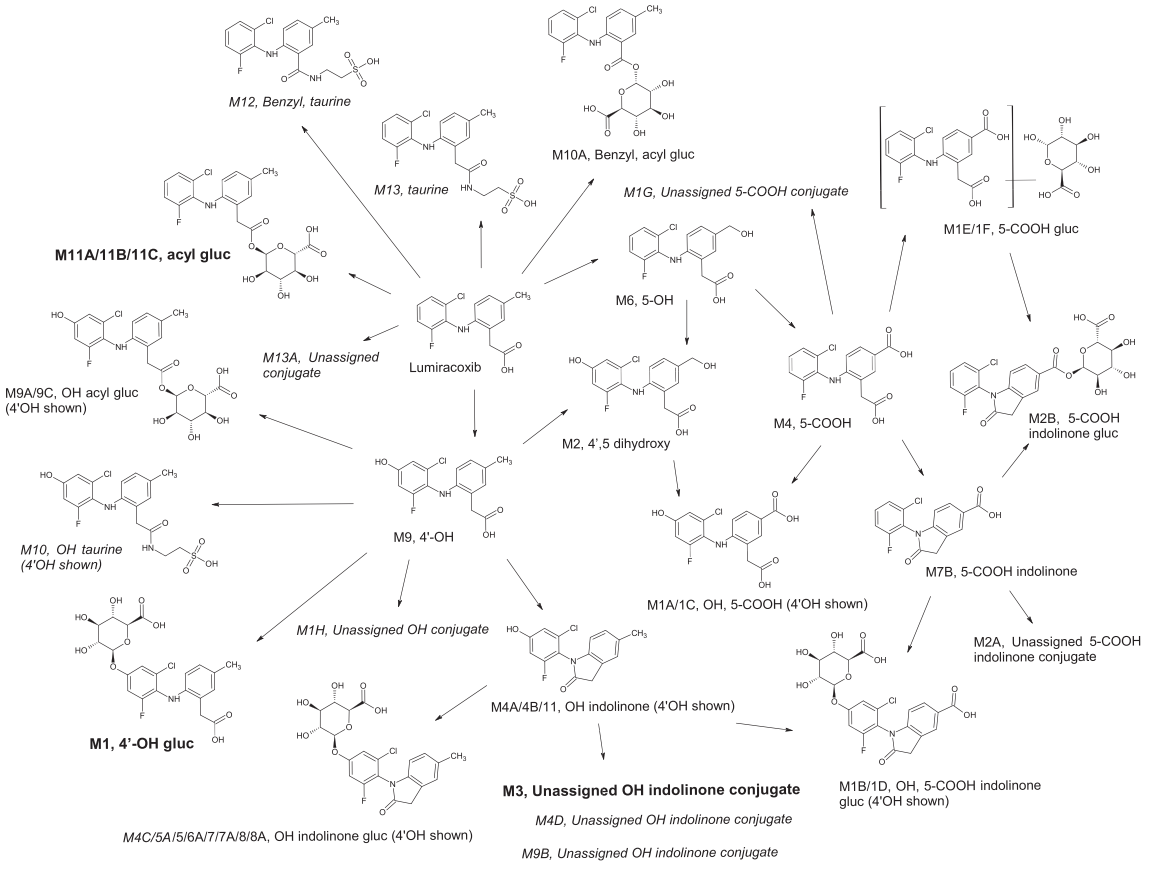

Fig. 6. Proposed metabolic pathway of lumiracoxib in Mu-FRG™ mice. Principal metabolites are designated with large bold font. Metabolites found in Mu-FRG™ mice but not in Hu-FRG™ mice are designated with italic font.

Please cite this article in press as: A.P. Dickie et al., The pharmacokinetics and metabolism of lumiracoxib in chimeric humanized and murinized FRG mice, Biochem. Pharmacol. (2017), http://dx.doi.org/10.1016/j.bcp.2017.03.015

Table 4
Comparison of lumiracoxib and its metabolites observed in excreta from a human ADME study [18], the present study with Hu-FRG™ and Mu-FRG™ mice, and wild type C57bl/6J mice [12].

Peak ID	Assignment	Human #	Hu-FRG™	Mu-FRG™	C57bl/6J ##
P	Lumiracoxib	++++	+++	+++	++
M1	4'-OH glucuronide	-	++	++++	++++
M1A	4'-OH, 5-COOH	++++*	++	-	-
M1B	4'-OH, 5-COOH indolinone glucuronide	+*	++	-	-
M1C	OH, 5-COOH	+++*	++	+	-
M1D	OH, 5-COOH indolinone glucuronide	+*	++	-	-
M1E	5-COOH glucuronide	++*	+++	-	-
M1F	5-COOH glucuronide	++*	+	-	-
H2	5-COOH, 4'-OH sulfate	++	-	-	-
H4/H6	5-COOH indolinone, 4'-OH sulfate	++	-	-	-
M1G	Unassigned 5-COOH conjugate	-	-	++	-
M1H	Unassigned OH conjugate	-	-	+++	-
M2	4',5 dihydroxy	+	++	++	+++
H8	4'-OH, 5-COOH indolinone	+++	-	-	-
M2A	Unassigned 5-COOH indolinone conjugate	-	++	+	-
M2B	5-COOH indolinone glucuronide	+++	+	++	-
M3	Unassigned OH indolinone conjugate	-	++	++++	++++
M4	5-COOH	++++	+	+	++
H12	4'-OH, 5-COOH indolinone, unassigned OH	+	-	-	-
H13	4'-OH, 5-COOH indolinone, unassigned OH glucuronide	+	-	-	-
M4A	OH indolinone	-	+	+	-
M4B	OH indolinone	-	++	+++	-
M4C	OH indolinone glucuronide	-	-	++	-
M4D	Unassigned OH indolinone conjugate	-	-	+++	-
M5	OH indolinone glucuronide	-	++	+++	++
M5A	OH indolinone glucuronide	-	-	++	-
M6	5-OH	+++	+++	+++	++++
M6A	OH indolinone glucuronide	-	++	+	-
M7	5-OH indolinone glucuronide	-	+++	+	+
M7A	OH indolinone glucuronide	-	++	++	-
M7B	5-COOH indolinone	+++	+	++	-
M7C	OH indolinone glucuronide	-	+	-	-
M8	4'-OH indolinone glucuronide	+	++	++	++
M8A	OH indolinone glucuronide	-	++	++	-
M9	4'-OH	+++	++	+++	+++
M9A	OH acyl glucuronide	-	++	++	-
M9B	Unassigned OH indolinone conjugate	-	-	+	-
M9C	OH acyl glucuronide	-	++	++	-
M10	OH taurine	-	-	+	++
M10A	Benzyl, acyl glucuronide	-	+	+	-
M11	OH indolinone	+++	+	+	++
M11A	Acyl glucuronide	-	++	++	-
M11B	Acyl glucuronide	-	+	+	-
M11C	1β-O-acyl glucuronide	+	++++	++++	-
M12	Benzyl, taurine	-	-	+	++
M13	Taurine	-	-	++	++
M13A	Unassigned conjugate	-	-	+	-

Key: ++++ detected > 5×10^5; +++ detected > 10^5; ++ detected > 10^4; + detected > 10^3, in the present study, or equivalent relative measures in the human and mouse studies; – not reported/below level of detection, * single metabolite observed in the human study may correspond to one or more metabolites observed in the present study. # [18], ## [12].

Please cite this article in press as: A.P. Dickie et al., The pharmacokinetics and metabolism of lumiracoxib in chimeric humanized and murinized FRG mice, Biochem. Pharmacol. (2017), http://dx.doi.org/10.1016/j.bcp.2017.03.015

It has been postulated that the hepatotoxicity seen for lumiracoxib in humans, as a result of which the drug was largely withdrawn from therapeutic use, resulted from the formation of reactive metabolites of the type observed for the structurally related drug diclofenac [e.g., 24–27]. Indeed Li et al. [8] showed that rat and human liver microsomes, as well as human hepatocytes, were capable of the in vitro biotransformation of the drug via a CYP2C9-mediated reaction to two N-acetylcysteinyl (NAC) conjugates (mercapturates). The structures of these mercapturates corresponded to 3′-NAC-4′-hydroxy lumiracoxib and the defluorinated 4′hydroxy-6′-NAC-desfluoro lumiracoxib (metabolic dehalogenation has also been reported in vitro for diclofenac [28]). However, neither of the two mercapturates (or structurally related metabolites) was detected in either the human radiolabelled metabolism study [18] nor in our own recent study in the C57bl/6J mouse [12]. Similarly, despite careful investigation of the urine, bile and faecal extract samples we detected no trace of these metabolites, nor evidence for metabolic defluorination, in the samples obtained from either the Hu-FRG™ or Mu-FRG™ mice in the present study. In the absence of evidence for reactive metabolites resulting from oxidative metabolism in these in vivo studies, and assuming that the toxicity of lumiracoxib observed in humans was the result of metabolic bioactivation, a potential candidate is the formation of chemically reactive acyl glucuronide conjugates. Acyl glucuronides have long been associated with drugs that cause DILI [29,30] and, at physiological pH, can undergo both hydrolysis and transacylation with the concomitant formation of stable adducts to proteins via a number of mechanisms [31]. In this study, the urinary profiles of the Hu-FRG™ mice were dominated by the lumiracoxib acyl glucuronide (M11C), with smaller amounts of the transacylated glucuronides such as M11A/B) also present. Whilst little is known concerning the reactivity of the lumiracoxib acyl glucuronide a number of investigations have shown covalent modification of proteins due to the acyl glucuronide of the structural analogue diclofenac. Thus, in studies in the rat using an anti-diclofenac antibody, diclofenac-modified proteins were detected on the canalicular membranes [32]. The formation of these adducts required functional Mrp2 to be present and was attributed to diclofenac acyl glucuronide. In addition, the acyl glucuronide of the NSAID zomepirac has been shown to form an adduct to rat dipeptidyl peptidase IV (DPP IV) that was identified (in vitro and in liver extracts) via immunoblotting [33]. The presence of this adduct suggested that DPP IV was one of the proteins covalently modified during the biliary excretion of the drug, and similar binding to DPP IV in rat liver has also been shown for diclofenac [34]. Evidence has also been reported for circulating drug-modified HSA in samples derived from patients who were administered diclofenac, where "at least a fraction of these modifications" was ascribed to the reactivity of the acyl glucuronide [35].

In comparing and contrasting the various metabolite profiles seen in the two varieties of chimeric mice and the C57bl/6J animals with respect to lumiracoxib metabolism in humans, as shown in both the mass chromatograms and summarized in the "Metmap" provided by Table 4, it is clear that there is a greater degree of similarity between the chimeric Hu-FRG™ mice and humans than for either the wild type or Mu-FRG™ mice. However, it is also clear that the Mu-FRG™ mice, whilst producing many of the same metabolites, were not equivalent to the C57bl/6J animals but also produced some metabolites seen in the profiles of the Hu-FRG™, as well as revealing a number of unique metabolites such as e.g., **M1G** (an unassigned 5-COOH conjugate) and **M1H** (an unassigned OH conjugate) (see Table 3).

The differences between the Mu-FRG™ and wild type C57bl/6J mice on the one hand, and the similarities between the Mu-FRG™ and Hu-FRG™ chimeric mice on the other are intriguing and beget a number of questions. It may well be that the generation of the FRG™ mouse (extraction, culturing and transplantation of the mouse) has resulted in an increased induction of extrahepatic enzymes, particularly in the gut wall, as suggested by the apparent lower oral AUC for the drug in both types of chimeric mouse.

However, there are, based on the LC–MS metabolite profiles determined here for the Hu-FRG™ and Mu-FRG™ mice clear qualitative differences between the two types of chimeric animal in the amounts of common, chimeric mouse-specific metabolites produced. Clearly, further investigations are warranted to determine the extent of extrahepatic metabolism of lumiracoxib in the mouse in order to shed light on these questions.

Determination of the metabolic fate of lumiracoxib in liver chimeric Hu-FRG™ mice using LC–MS indicates that the former provides a metabolic profile that recapitulates the human metabolism of the drug more faithfully than either Mu-FRG™ chimeric or wild type C57bl/6J mice. Simply, in terms of metabolites produced, the Mu-FRG™ appeared to be somewhat intermediate between the C57bl/6J mouse and the Hu-FRG™ chimera, but there were also significant qualitative differences. Despite careful interrogation of the LC–MS data, neither defluorinated metabolites nor metabolites indicative of the formation of reactive metabolites, such as mercapturates, were detected in either blood or the excreta of either the Hu-FRG™ or Mu-FRG™ mice in the present study, as was the case in our previous study in the C57bl/6J mouse [12]. Overall, whilst some differences were observed between the metabolism of lumiracoxib in Hu-FRG™ chimeric mice and that in humans, these were relatively minor and, as a result, may offer a more useful predictive model for human metabolism than other preclinical species.

Conflict of interest

The authors declare no financial or commercial conflict of interest.

References

[1] I. Kola, J. Landis, Can the pharmaceutical industry reduce attrition rates? Nat. Rev. Drug Discovery 3 (2004) 711–716.
[2] M.J. Waring, J. Arrowsmith, A.R. Leach, P.D. Leeson, S. Mandrell, R.M. Owen, et al., An analysis of the attrition of drug candidates from four major pharmaceutical companies, Nat. Rev. Drug Discovery 14 (2015) 475–486.
[3] N. Kaplowitz, Idiosyncratic drug hepatotoxicity, Nat. Rev. Drug Discov. 4 (2005) 489–499.
[4] J.R. Senior, Drug hepatotoxicity from a regulatory perspective, Clin. Liver Dis. 11 (2007) 507–524.
[5] S. Chitturi, G.C. Farrell, Identifying who is at risk of drug-induced liver injury: is human leukocyte antigen specificity the key? Hepatology 53 (2011) 358–362.
[6] B. Bannwarth, F. Berenbaum, Lumiracoxib in the management of osteoarthritis and acute pain, Expert Opin. Pharmacother. 8 (2007) 1551–1564.
[7] A. Buvanendran, R. Barkin, Lumiracoxib, Drugs Today 43 (2007) 137–147.
[8] Y. Li, J.G. Slatter, Z. Zhang, Y. Li, G.A. Doss, M.P. Braun, et al., In vitro metabolic activation of lumiracoxib in rat and human liver preparations, Drug Metab. Dispos. 36 (2008) 469–473.
[9] J.B. Singer, S. Lewitzky, E. Leroy, F. Yang, X. Zhao, L. Klickstein, et al., A genome-wide study identifies HLA alleles associated with lumiracoxib-related liver injury, Nat. Genet. 42 (2010) 711–714.
[10] N.C. Teoh, G.C. Farrell, Hepatotoxicity associated with non-steroidal anti-inflammatory drugs, Clin. Liver Dis. 7 (2003) 401–413.
[11] P. Kang, D. Dalvie, E. Smith, M. Renner, Bioactivation of lumiracoxib by peroxidases and human liver microsomes: identification of multiple quinone imine intermediates and GSH adducts, Chem. Res. Toxicol. 22 (2009) 106–117.
[12] A.P. Dickie, C.E. Wilson, K. Schreiter, R. Wehr, I.D. Wilson, R.J. Riley, Lumiracoxib metabolism in male C57bl/6J mice: characterisation of novel in vivo metabolites, Xenobiotica (2016), http://dx.doi.org/10.1080/00498254.2016.1206239.
[13] H. Azuma, N. Paulk, A. Ranade, C. Dorrell, M. Al-Dhalimy, E. Ellis, et al., Robust expansion of human hepatocytes in Fah-/-/Rag2-/-/Il2rg-/- mice, Nat. Biotechnol. 25 (2007) 903–910.
[14] H. Kamimura, N. Nakada, K. Suzuki, A. Mera, K. Souda, Y. Murakami, et al., Assessment of chimeric mice with humanized liver as a tool for predicting circulating human metabolites, Drug Metab. Pharmacokinet. 25 (2010) 223–235.

Please cite this article in press as: A.P. Dickie et al., The pharmacokinetics and metabolism of lumiracoxib in chimeric humanized and murinized FRG mice, Biochem. Pharmacol. (2017), http://dx.doi.org/10.1016/j.bcp.2017.03.015

[15] S.C. Strom, J. Davila, M. Grompe, Chimeric mice with humanized liver: tools for the study of drug metabolism, excretion, and toxicity, Methods Mol. Biol. 640 (2010) 491–509.
[16] N. Scheer, I.D. Wilson, A comparison between genetically humanized and chimeric liver humanized mouse models for studies in drug metabolism and toxicity, Drug Discovery Today 21 (2016) 250–263.
[17] S. Sarda, C. Page, K. Pickup, T. Schulz-Utermoehl, I. Wilson, Diclofenac metabolism in the mouse: novel in vivo metabolites identified by high performance liquid chromatography coupled to linear ion trap mass spectrometry, Xenobiotica 42 (2012) 179–194.
[18] J.B. Mangold, H. Gu, L.C. Rodriguez, J. Bonner, J. Dickson, C. Rordorf, Pharmacokinetics and metabolism of lumiracoxib in healthy male subjects, Drug Metab. Dispos. 32 (2004) 566–571.
[19] M.J. Galmier, B. Bouchon, J.C. Madelmont, F. Mercier, F. Pilotaz, C. Lartigue, Identification of degradation products of diclofenac by electrospray ion trap mass spectrometry, J. Pharm. Biomed. Anal. 38 (2005) 790–796.
[20] T. Kosjek, E. Heath, S. Perez, M. Petrovic, D. Barcelo, Metabolism studies of diclofenac and clofibric acid in activated sludge bioreactors using liquid chromatography with quadrupole – time-of-flight mass spectrometry, J. Hydrol. 372 (2009) 109–117.
[21] M.P. Grillo, C.G. Knutson, P.E. Sanders, D.J. Waldon, F. Hua, J.A. Ware, Studies on the chemical reactivity of diclofenac acyl glucuronide with glutathione: identification of diclofenac-S-acyl-glutathione in rat bile, Drug Metab. Dispos. 31 (2003) 1327–1336.
[22] H. Stierlin, J.W. Faigle, A. Sallmann, W. Küng, W.J. Richter, H.P. Kriemler, et al., Biotransformation of diclofenac sodium (Voltaren) in animals and in man. I. Isolation and identification of principal metabolites, Xenobiotica 9 (1979) 601–610.
[23] M.P. Grillo, J. Ma, Y. Teffera, D.J. Waldon, A novel bioactivation pathway for 2-[2-(2,6-dichlorophenyl)aminophenyl]ethanoic acid (diclofenac) initiated by cytochrome P450-mediated oxidative decarboxylation, Drug Metab. Dispos. 36 (2008) 1740–1744.
[24] G.K. Poon, Q. Chen, Y. Teffera, J.S. Ngui, P.R. Griffin, M.P. Braun, et al., Bioactivation of diclofenac via benzoquinone imine intermediates – identification of urinary mercapturic acid derivatives in rats and humans, Drug Metab. Dispos. 29 (2001) 1608–1613.
[25] W. Tang, R.A. Stearns, S.M. Bandiera, Y. Zhang, C. Raab, M.P. Braun, et al., Studies on cytochrome P-450-mediated bioactivation of diclofenac in rats and in human hepatocytes: identification of glutathione conjugated metabolites, Drug Metab. Dispos. 27 (1999) 365–372.
[26] W. Tang, The metabolism of diclofenac: enzymology and toxicology perspectives, Curr. Drug Metab. 4 (2003) 319–329.
[27] D.J. Waldon, Y. Teffera, A.E. Colletti, J. Liu, D. Zurcher, K.W. Copeland, et al., Identification of quinone imine containing glutathione conjugates of diclofenac in rat bile, Chem. Res. Toxicol. 23 (2010) 1947–1953.
[28] L.J. Yu, Y. Chen, M.P. De Ninno, T.N. O'Connell, C.E. Hop, Identification of a novel glutathione adduct of diclofenac, 4′-hydroxy-2′-glutathion-deschloro-diclofenac, upon incubation with human liver microsomes, Drug Metab. Dispos. 33 (2005) 484–488.
[29] A.V. Stachulski, J.R. Harding, J.C. Lindon, J.L. Maggs, B.K. Park, I.D. Wilson, Acyl glucuronides: biological activity, chemical reactivity, and chemical synthesis, J. Med. Chem. 2006 (49) (2006) 6931–6945.
[30] S.L. Regan, J.L. Maggs, T.G. Hammond, C. Lambert, D.P. Williams, B.K. Park, Acyl glucuronides: the good, the bad and the ugly, Biopharm. Drug Dispos. 31 (2010) 367–395.
[31] R.N. Monrad, J.C. Errey, C.S. Barry, M. Iqbal, X. Meng, L. Iddon, et al., Dissecting the reaction of Phase II metabolites of ibuprofen and other NSAIDS with human plasma protein, Chem. Sci. 5 (2014) 3789–3794.
[32] S. Seitz, A. Kretz-Rommel, R.P. Oude Elferink, U.A. Boelsterli, Selective protein adduct formation of diclofenac glucuronide is critically dependent on the rat canalicular conjugate export pump (Mrp2), Chem. Res. Toxicol. 11 (1998) 513–519.
[33] M. Wang, M.D. Gorrell, G.W. McGaughan, R.G. Dickinson, Dipeptidyl peptidase IV is a target for covalent adduct formation with the acyl glucuronide metabolite of the anti-inflammatory drug zomepirac, Life Sci. 68 (2001) 785–797.
[34] S.J. Hargus, B.M. Martin, J.W. George, L.R. Pohl, Covalent modification of rat liver dipeptidyl peptidase IV (CD26) by the nonsteroidal anti-inflammatory drug diclofenac, Chem. Res. Toxicol. 8 (1995) 993–996.
[35] T.G. Hammond, X. Meng, R.E. Jenkins, J.L. Maggs, A.S. Castelazo, S.L. Regan, et al., Mass spectrometric characterization of circulating covalent protein adducts derived from a drug acyl glucuronide metabolite: multiple albumin adductions in diclofenac patients, Pharmacol. Exp. Ther. 350 (2014) 387–402.

Please cite this article in press as: A.P. Dickie et al., The pharmacokinetics and metabolism of lumiracoxib in chimeric humanized and murinized FRG mice, Biochem. Pharmacol. (2017), http://dx.doi.org/10.1016/j.bcp.2017.03.015